Features of ω photoproduction off proton target at backward angles: Role of nucleon Reggeon in u-channel with parton contributions

Byung-Geel Yu* and Kook-Jin Kong†

Research Institute of Basic Science, Korea Aerospace University, Goyang 10540, Korea

(Received 5 November 2018; published 24 January 2019)

Backward photoproduction of ω off a proton target is investigated in a Reggeized model where the u-channel nucleon Reggeon is constructed from the nucleon Born terms in a gauge invariant way. The t-channel meson exchanges are considered as a background. While the N_α trajectory of the nucleon Reggeon reproduces the overall shape of NINA data measured at the Daresbury Laboratory in the range of u-channel momentum transfer squared $-1.7 < u < 0.02$ GeV^2 and energies at $E_\gamma = 2.8$, 3.5, and 4.7 GeV, a possibility of parton contributions is searched for through the nucleon isoscalar form factor which is parametrized in terms of parton distributions at the ωNN vertex. A detailed analysis is presented for NINA data to understand the reaction mechanism that could fill up the deep dip from the nucleon Reggeon at momentum squared $u = -0.15$ GeV^2. The angle dependence of differential cross sections at the NINA energies above are reproduced in the overall range of u including the CLAS data at forward angles as well. The energy dependence of the differential cross section is investigated based on the NINA data and the recent LEPS data. A feature of the present approach that implicates parton contributions via the nucleon form factor is illustrated in the total and differential cross sections provided by GRAAL and CB-ELSA Collaborations.

DOI: 10.1103/PhysRevD.99.014031

I. INTRODUCTION

Understanding the structure of hadrons based on QCD is a longstanding issue and hadron reactions at wide angles are a useful means to investigate parton contributions to reaction processes. In search of parton distributions in hadrons, the recent experimental activities and theoretical developments have been concentrated on identifying the scaling of cross sections for meson photo/electroproductions at mid angle [1–5] as well as the hadron form factors in terms of parton densities at large virtual photon momentum squared [6–8].

In photoproductions of lighter vector mesons ρ, ω, and ϕ, the peripheral scattering of mesons and Pomeron exchanges is suppressed at large angles, but an enhancement of quark exchange is expected due to the smaller impact parameter $\sim 1/\sqrt{-t}$. Scaling of differential cross sections for hadron reactions with respect to energy is one of the examples that perturbative QCD predicts at mid angle $\theta \approx 90°$ [1]. The possibilities of such hard processes were examined in the CLAS experiment where the differential cross sections of ω photoproduction were measured over the resonance region $2.6 < W < 2.9$ GeV up to the momentum transfer squared $-t = 5$ GeV^2 [9]. Around the mid angle $\theta \approx 90°$ the scaling of cross sections by s^8 in the photon energy $E_\gamma = 3.38$–3.56 GeV seems to be consistent with quark and gluon exchanges predicted by the QCD-inspired model [10] as well as the Reggeized meson exchanges in the t-channel with the trajectory saturated at large $-t$ [11–14].

At very backward angles $\theta \approx 180°$ beyond resonances, however, theory and experiment in this kinematical region are rare [9,10,15–18] and only the data from the NINA electron synchrotron at the Daresbury Laboratory [17] are available at present for the u-channel momentum squared $-1.8 < u < 0.02$ GeV^2 at $E_\gamma = 2.8$–4.7 GeV. Because of the isoscalar nature of the ω meson it is expected that the reaction at backward angles is dominated by the u-channel nucleon exchange with a dip at $u = -0.15$ GeV^2 arising from the nonsense wrong signature zero (NWSZ) of the N_α trajectory. Interestingly enough, however, the measured cross section exhibited the dip much weaker than predicted by the Regge theory, and hence, a sort of a mechanism is needed to fill up the depth of the dip. While there are no other baryon trajectories to play such a role, the authors of Ref. [17] suggested a possibility of parton contributions there by showing the s^8 scaling of the cross section over the

*bgyu@kau.ac.kr
†kong@kau.ac.kr

dip in the analysis of data at $E_\gamma = 3.5$ GeV. The s^8 scaling is also experimentally observed in ρ^0 photoproduction [19].

Meanwhile, as the scaling of the cross section for meson photoproduction is mostly due to quark and gluon dynamics through the hard process at mid angle [2,3], it becomes, therefore, a significant issue how to understand the recurrence of the scaling by parton contributions at very backward angles, i.e., $155° < \theta < 163°$ in the range $2.8 < E_\gamma < 4.8$ GeV, which corresponds to $-0.2 < u < -0.1$ GeV^2, as they claimed.

Recently this issue was reexamined in Ref. [15] to investigate backward ω photoproduction in the baryon pole model with hadron form factors considered. However, the discussion on the reaction mechanism around the expected dip, as well as its appearance in the data, was no longer valid in the model because the occurrence of a dip is a unique feature of the baryon trajectory at the NWSZ in the Regge theory. Thus, the production mechanism of ω photoproduction at very backward angles remains not fully understood yet, and the topic raised by the NINA data should be revisited within the Regge framework for the u-channel nucleon exchange.

In this work we study backward ω photoproduction with our interest in the search of the hard process [10] involved in the NINA data [17]. We attempt to explain the two experimental observations: the disappearance of the dip of nucleon trajectory at the particular momentum and the possibility of s^8 scaling of the differential cross section there by parton contributions. In order to examine whether the recurrence of scaling by parton contributions is feasible at very backward angles or not, we consider an extension of the Regge amplitude to include parton distributions for the analysis of the isotropic NINA data observed in the very backward region.

This paper is organized as follows: Section II is devoted to a construction of the photoproduction amplitude where the nucleon exchange is Reggeized with the background contribution from the meson exchanges. Discussion is given on how to consider parton contributions in the hadronic production amplitude. In Sec. III numerical consequences in the differential cross sections are presented to compare with existing data. More proofs for the validity of the present approach to current issues are given in the differential and total cross sections in the region where the nucleon Reggeon plays a role. A summary and discussions follow in Sec. IV.

II. BARYON REGGEON MODEL

At backward angles where the u-channel momentum squared $|u|$ is small, hadron reactions are well described by the u-channel baryon Reggeon in the resonance region [20]. In this section we discuss a construction of the photoproduction amplitude for the nucleon Reggeon because the isoscalar ω prohibits baryon resonances of isospin $I = 3/2$ from the $\gamma p \to \omega p$ reaction. In the Reggeization of the relativistic Born terms, the nucleon exchange in the u-channel alone is not gauge invariant due to the charge coupling term and the nucleon exchange in the s-channel is introduced further to preserve the gauge invariance of the production amplitude.

At higher energies beyond the resonance region, the meson exchange in the t-channel begins to give a contribution. To reproduce experimental data in the overall range of energy and angle, therefore, it is necessary to include the meson exchange as a background contribution. However, in order to avoid the possibility of double counting caused by the s- and t-channel duality, we consider the t-channel meson exchange as a simple pole with the cutoff function for the divergence of the cross section at high energies.

A. Nucleon exchange Reggeized in the u-channel

For the gauge invariance of the nucleon exchange, as shown in Fig. 1, we now write the nucleon Born terms as

$$M_s = \bar{u}(p')\Gamma_{\omega NN}\frac{\not{p}+\not{k}+M_N}{s-M_N^2}\Gamma_{\gamma NN}u(p), \tag{1}$$

$$M_u = \bar{u}(p')\Gamma_{\gamma NN}\frac{\not{p}'-\not{k}+M_N}{u-M_N^2}\Gamma_{\omega NN}u(p), \tag{2}$$

where the electromagnetic and strong coupling vertices are given by

$$\Gamma_{\gamma NN} = e\left(e_N\not{\epsilon} - \frac{\kappa_N}{4M_N}[\not{\epsilon},\not{k}]\right), \tag{3}$$

$$\Gamma_{\omega NN} = g_{\omega NN}\left(\not{\eta}^* + \frac{\kappa_\omega}{4M_N}[\not{\eta}^*,\not{q}]\right), \tag{4}$$

where $u(p)$, $\bar{u}(p')$ are Dirac spinors of the initial and final nucleons with momenta p and p', and ϵ^μ and $\eta^{\nu*}$ are polarization vectors of incoming photon and outgoing ω with momenta k and q. The charge and anomalous magnetic moments are $e_N = 1$, $\kappa_N = 1.79$ for proton and $e_N = 0$, $\kappa_N = -1.91$ for neutron. We take $g_{\omega NN} = 15.6$ by the universality of the ω meson decay constant f_ω, and

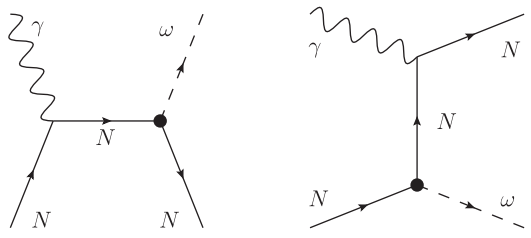

FIG. 1. Nucleon Born terms in the s- and u-channels. Blobs at the ωNN vertices indicate inclusion of the nucleon isoscalar form factor in addition to the point coupling interaction in Eq. (14).

$\kappa_\omega = 0$ for consistency with the results from the other hadronic process, $\gamma N \to \pi^0 N$, for instance [11].

The Reggeization of the u-channel amplitude is simply done by replacing the u-channel pole $(u - M^2)$ with the nucleon Regge propagator $\mathcal{R}^N(s,u)$ in the gauge invariant nucleon pole terms, and the Reggeized amplitude is expressed as

$$\mathcal{M}_N = [M_s + M_u] \times (u - M_N^2)\mathcal{R}^N(s,u), \tag{5}$$

with $\mathcal{R}^N(s,u)$ given by

$$\mathcal{R}^N(s,u) = \frac{\pi\alpha'_N}{\Gamma(\alpha_N(u)+0.5)} \frac{(1+\tau e^{-i\pi(\alpha_N(u)-0.5)})}{2\sin\pi(\alpha_N(u)-0.5)} \times \left(\frac{s}{s_0}\right)^{\alpha_N(u)-0.5}. \tag{6}$$

Here, the signature is defined as $\tau = (-)^{J-1/2}$ and $\tau = 1$ for nucleon. $s_0 = 1$ GeV^2.

Given the baryon trajectory of the form for the spin J

$$\alpha(\sqrt{u}) = \alpha' u + \alpha_0, \tag{7}$$

the MacDowell symmetry predicts the existence of the state with the same signature τ but the opposite parity. Thus, denoting $\alpha^+(\sqrt{u}) = \alpha^-(-\sqrt{u})$ to distinguish the states between the same spin but opposite parities, the nonexistence of the parity negative state corresponding to the nucleon in the Chew-Frautschi plot should dictate $1 + e^{-i\pi(\alpha_N(u)(\sqrt{u})-0.5)} = 0$ in order not to contribute to the reaction process. This leads to an occurrence of a dip by the NWSZ at some position of u.

In accordance with many applications we take the slope $\alpha' = 0.9$ GeV^{-2}. But the value for the intercept α_0 in the literature varies in the range around -0.3. Here, we choose $\alpha_0 = -0.365$ so that the trajectory in Eq. (7) yields the dip at $u = -0.15$ GeV^2 measured in the NINA data at $E_\gamma = 2.8$, 3.5, and 4.7 GeV [17].

B. Meson poles in t-channel as a background

Now that the nucleon Reggeon in the u-channel in Eq. (5) gives the contribution, in general, by an order of magnitude smaller than that of the π exchange in the t-channel, it is not enough to reproduce the cross section data solely by the nucleon Reggeon contribution in the overall range of angles. Therefore, we consider the contributions of meson exchanges together with the Pomeron as a background on which the nucleon Reggeon is based.

Given the nucleon Reggeon $\mathcal{M}_N$ in Eq. (5), the production amplitude for the exchanges of the natural and unnatural parity mesons consists of the following two terms:

$$\mathcal{M}_{\rm nat} = \mathcal{M}_N + \mathcal{M}_\sigma + \mathcal{M}_{f_2} + \mathcal{M}_{\mathbb{P}}, \tag{8}$$

$$\mathcal{M}_{\rm unnat} = \mathcal{M}_\pi + \mathcal{M}_{f_1}, \tag{9}$$

respectively. For consistency with our previous work, we utilize the meson exchanges with coupling constants taken the same as in Ref. [14]. As discussed above, the meson exchanges in Ref. [14] are now given as the t-channel poles with the pole propagator,

$$(t - m_\varphi^2)^{-1} \tag{10}$$

and the cutoff function of the type

$$\left(\frac{\Lambda_\varphi^2 - m_\varphi^2}{\Lambda_\varphi^2 - t}\right)^n \tag{11}$$

for $\varphi = \pi$, σ, and f_1. As for the f_2 exchange, however, due to the highly divergent behavior, despite the large cutoff mass, we employ it as the t-channel Reggeon. Though an inconsistent treatment with other mesons, it is not subject to the double counting between the u-channel Reggeon and the t-channel exchanges including f_2 Reggeon, because the double counting by the t-channel Reggeon holds with the s-channel baryon resonances, but not with the u-channel Reggeon.

To fix the cutoff mass Λ_φ in Eq. (11) we exploit the natural and unnatural parity cross sections over the resonance region. Before doing this, however, it should be cautioned that the determination of the sign of the π exchange relative to the nucleon is of importance, because these two are the leading contributions to the reaction at forward and backward angles, respectively.

In Fig. 2(a), by adjusting the cutoff $\Lambda_\sigma = 0.65$ GeV, we find that the coupling constant $g_{\omega NN} = +15.6$ gives a good fit to the natural parity cross section. By using $\Lambda_{f_1} = 1.3$ GeV for f_1 and $\Lambda_\pi = 0.72$ GeV with $n = 2$ to suppress the large coupling at the $\gamma\pi\omega$ vertex, a fair agreement is obtained as shown in Fig. 2(b). For further confirmation of the coupling constants and cutoff masses chosen above, we will provide differential and total cross sections at low energies in the following section for numerical consequences. We summarize the coupling constants and cutoff masses in Table I.

C. Parton contribution and scaling

Since our interest is in the analysis of the reaction mechanism which is suggestive of the hard process at very small $-u$, we proceed to consider parton contributions in the hadronic amplitude in Eqs. (8) and (9).

The differential cross section for the u-channel momentum transfer squared is defined as

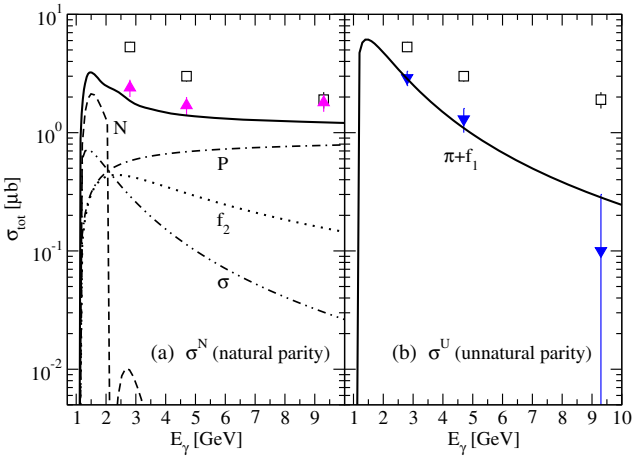

FIG. 2. Natural and unnatural parity cross sections for $\gamma p \to \omega p$. The dashed curve is from the proton Reggeon with a sequence of the dip from the N_α trajectory. $\kappa_p = 1.79$, $g_{\omega NN} = 15.6$, $\kappa_\omega = 0$ are taken in Eqs. (3) and (4). In (b), the solid curve is from the π exchange with f_1 of the 10^{-5} order contribution. Data are taken from Ref. [21].

$$\frac{d\sigma}{du} = \frac{M_N^2}{16\pi(s-M_N^2)^2}\frac{1}{4}\sum_{\text{spins}}|\mathcal{M}|^2. \tag{12}$$

The NINA data from the reaction $\gamma p \to \omega p$ at $E_\gamma = 3.5$ GeV are analyzed by a parametrization of $d\sigma/du$ which is divided by hadronic and hard scattering parts, respectively [17], i.e.,

$$\frac{d\sigma}{du} = |A(u)s^{\alpha(u)-1} + B(u)e^{i\phi(u)}s^{-n/2}|^2. \tag{13}$$

Then, a fit of data with the s^8 scaling assumed in the hard scattering term produces the $B(u)$ isotropic at the relative angle $\phi \simeq 90°$ for all u. This suggests incoherency between the hadronic process and hard scattering [17]. More analysis [17] leads us to interpret the hadronic term as the Reggeon with energy dependence $s^{\alpha-1}$, in which case the trajectory $\alpha(u)$ generates a typical dip at the expected position. The $B(u)$-term in the hard scattering is regarded as parton contributions with s^8 scaling with respect to the momentum squared u.

TABLE I. Physical constants of exchanged mesons and parameters for form factors. Masses and cutoff parameters are given in units of MeV. The f_2 Reggeon has no form factor and the Pomeron is taken from Ref. [14].

Meson	Mass	n	Λ_φ	$g_{\gamma\varphi\omega}$	$g_{\varphi NN}$
π	134.977	2	720	−0.69	13.4
σ	500	1	650	−0.17	14.6
f_1	1281.9	1	1300	0.18	2.5
f_2	1275.1	⋯	⋯	0.0376	6.45

In order to include the parton contributions in the hadronic amplitude it is natural to suppose a possibility of parton distribution in nucleon form factors at very backward angles [7] in addition to the point coupling of the ωNN vertex in Eq. (4), as depicted in Fig. 2. For this we introduce the isoscalar form factor $F^{(s)}(u)$ of the nucleon by the similarity of the ωNN vertex to a virtual photon coupling, $\gamma^* NN$. Therefore, the ωNN vertex in the nucleon Reggeon in Eq. (5) is extended to include the additional coupling, i.e.,

$$g_{\omega NN}\gamma^\nu\left(\frac{s}{s_0}\right)^{\alpha_N(u)} \to g_{\omega NN}\left[\gamma^\nu\left(\frac{s}{s_0}\right)^{\alpha_N(u)} + e^{i\phi(u)}\gamma^\nu F^{(s)}(u)\left(\frac{s}{s_0}\right)^{\tilde{\alpha}_N(u)}\right] \tag{14}$$

with the relative angle $e^{i\phi(u)}$ between the two coupling phases. As a result, the nucleon Reggeon is extended to include parton contributions via the nucleon isoscalar form factor, $\mathcal{R}^N \to (\mathcal{R}^N + e^{i\phi(u)}F^{(s)}(u)\tilde{\mathcal{R}}^N)$, and we write the full amplitude as

$$\mathcal{M} = (\mathcal{M}_N + \mathcal{M}_{\text{b.g.}}) + e^{i\phi}\tilde{\mathcal{M}}_N, \tag{15}$$

in accordance with Eq. (13) with the two terms in the bracket referring to hadronic contribution and the last to parton contributions, respectively. The term $\mathcal{M}_{\text{b.g.}}$ represents the background coming from all the meson exchanges in the t-channel, i.e., all terms excluding the nucleon term $\mathcal{M}_N$ in Eqs. (8) and (9). In the additional Reggeon $\tilde{\mathcal{M}}_N$, which has the parton contributions via the form factor, we further assume that the nucleon trajectory $\alpha_N(u)$ is modified to $\tilde{\alpha}_N(u)$ in the presence of parton dynamics at very small $|u|$.

The relative angle $e^{i\phi(u)}$ between hadronic and partonic phases is parametrized as a linear function of u

$$\phi(u) = (au + b)\frac{\pi}{180} \tag{16}$$

with a in units of GeV^{-2}.

The nucleon isoscalar form factor is composed of proton and neutron charge form factors [22]

$$F^{(s)} = F_1^p + F_1^n, \tag{17}$$

and in the parton model the quark contents of these are expressed as

$$F_1^p = e_u u + e_d d, \qquad F_1^n = e_u d + e_d u \tag{18}$$

with the quark distribution [7]

$$q(u) = \int dx q_v(x) x^{-(1-x)\alpha'(u-u_0)} \tag{19}$$

for the valence quarks u and d. Here, we favor to choose the ansatz for the momentum fraction x dependence of partons which simulates the Regge trajectory with the slope α' in units of GeV^{-2}, because of the relevance to the present formalism. However, we do not expect that the ansatz for the quark distribution in Eq. (19) could yield a risk of double counting by encoding the power of x similar to the Regge trajectory, because of the relative angle $\phi \simeq \pi/2$, which guarantees noninterference of the second term in Eq. (14) with the first one for whatever ansatz the parton contribution is involved. Nevertheless, in the case that numerical results are not exactly at $\phi = \pi/2$, but around it for a better fit, they might contain double counting between the two terms as much as the angle ϕ is deviated from $\pi/2$. The momentum squared u_0 is the maximum value of u to avoid a rapid divergence in the region $u > 0$ and α' is considered to be a parameter chosen for the calculation. As to the valence quark $q_v(x)$ we employ the unpolarized parton distributions for u and d quarks which are

$$u_v = 0.262x^{-0.69}(1-x)^{3.5}(1+3.83x^{0.5}+37.65x), \quad (20)$$

$$d_v = 0.061x^{-0.65}(1-x)^{4.03}(1+49.05x^{0.5}+8.65x), \quad (21)$$

at the input scale $\mu^2 = 1$ GeV^2, respectively. In the fitting procedure for the relative angle $\phi(u)$ and the trajectory $\tilde{\alpha}_N(u)$ to the NINA data we make the slope parameter adjusted to obtain $\alpha' = 0.3$ for a better result.

The sensitivity of the proton isoscalar form factor $F^{(s)}(u)$ to the slope parameter α' is examined to discuss its implication to physical processes. In Fig. 3 the form factor with $\alpha' = 0.3$ chosen here is compared to the case with $\alpha' = 1.105$ that is obtained from the fit of the proton Dirac form factor F_1^p to empirical data [23]. (We mean that the dependence of the form factor upon the momentum squared u is the same as the case upon the virtual photon momentum squared Q^2.) Given a contribution stronger than the case with 1.105, as shown, the choice of $\alpha' = 0.3$ largely deviates from the empirical form factor with $\alpha' = 1.105$ for the on-mass shell. In an application to hadron reactions just like the ω photoproduction, however, in order to agree with the differential data at $u = -0.15$ GeV^2, the slope $\alpha' = 0.3$ is favored rather than the case of 1.105. This is similar to the proton Dirac form factor $F_1^p(Q^2)$ in electroproduction $\gamma^* p \to \pi^+ n$ [23], in which case it is advantageous for the dipole fit of the form factor with the cutoff mass $\Lambda = 1.55$ GeV to agree with electroproduction data rather than the form factor with $\alpha' = 1.105$. Our choice of $\alpha' = 0.3$ yields the form factor which lies between the dipole form factor above and the one prescribed by Kaskulov and Mosel [24]. We regard these results to be feasible, because the form factor in the hadron reactions is, in general, half off shell, and needs not be the same as the on-shell one.

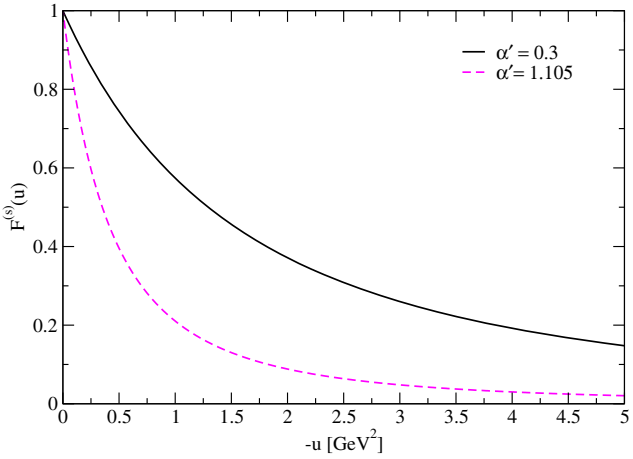

FIG. 3. u dependence of the proton isoscalar form factor $F^{(s)}(u)$. The solid curve results from $\alpha' = 0.3$ GeV^{-2} chosen for the present work and dashed curve results from $\alpha' = 1.105$ GeV^{-2} used for the fit of the proton Dirac form factor $F_1^p(Q^2)$ in the electroproduction $p(\gamma^*, \pi^+ n)$ [7].

III. NUMERICAL RESULTS

In the fitting procedure to NINA data, our practical purpose is how to fill up such a deep dip as shown by the dotted curve that results from the nucleon Reggeon $\mathcal{M}_N$ in Fig. 4(a) and how to simulate the scaling behavior of the cross section with respect to the momentum squared u

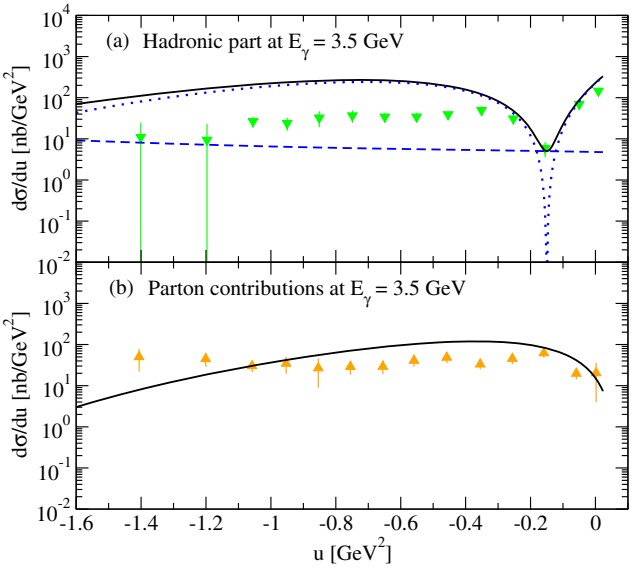

FIG. 4. Differential cross section for $\gamma p \to \omega p$ at $E_\gamma = 3.5$ GeV in accordance with Eq. (13). The curve in (a) results from the hadronic contribution consisting of the nucleon Reggeon, $\mathcal{M}_N$ (dotted curve), with the t-channel meson-pole exchange, $\mathcal{M}_{\text{b.g.}}$ (dashed). The curve in (b) shows the result of $\tilde{\mathcal{M}}_N$ in Eq. (15) with $\tilde{\alpha}_N = 0.9u - 0.56$ and the parton distributions in the $F^{(s)}(u)$ form factor given in the text. Data are taken from Ref. [17].

in 4(b) with parton contributions from the nucleon Reggeon $\tilde{\mathcal{M}}_N$ in addition. However, there is no evidence for a dip in the cross section of 4(b) for which the additional Reggeon $\tilde{\mathcal{M}}_N$ is applied, while it should produce a dip at the same place of u by the NWSZ of the trajectory $\tilde{\alpha}_N(u)$, unless it is different from the $\alpha_N(u)$. Thus, we have to move the position of the dip by $\tilde{\mathcal{M}}_N$ to another place by altering the trajectory $\tilde{\alpha}_N$ in Eq. (14). We let the trajectory of the $\tilde{\mathcal{R}}^N$ vary in the fitting procedure to obtain

$$\tilde{\alpha}_N(u) = 0.9u - 0.56 \tag{22}$$

with the intercept adjusted for the best fit to the NINA data in the overall range of the energy and angle. The dip position of $\tilde{\mathcal{R}}^N$ is now at $u = +0.067$ GeV^2, and hence, not appearing in the kinematical region of the reaction $u < 0.02$ GeV^2 so that the resulting cross section in 4(b) could simulate the scaling without a dip, as shown by the solid curve.

Given the differential cross section $d\sigma/du$ for $\gamma p \to \omega p$ at $E_\gamma = 3.5$ GeV separately into two parts as in Eq. (13), the hadronic contribution corresponding to the $s^{\alpha(u)-1}$-term and the s^{-8} scaling by parton contributions is shown in Figs. 4(a) and 4(b), respectively. In 4(a) the solid curve results from the sum of the dotted curve by the nucleon Reggeon and the dashed one by the t-channel meson exchanges, i.e., from the hadronic amplitude $\mathcal{M}_N + \mathcal{M}_{\text{b.g.}}$ in Eq. (15). As expected, the Reggeon $\mathcal{M}_N$ produces the deep dip at $u = -0.15$ GeV^2 some part of which could be covered over with the meson contribution. Nevertheless, the dip remains not fully compensated yet. Moreover, the solid curve of the hadronic contributions $\mathcal{M}_N + \mathcal{M}_{\text{b.g.}}$ is overestimating the data over 0.3 GeV$^2 < |u|$, which should be reduced. In 4(b) the solid curve is from the additional Reggeon, $\tilde{\mathcal{M}}_N$ with the trajectory $\tilde{\alpha}_N(u) = 0.9u - 0.56$ with the dip at $u = +0.067$ GeV^2 so that the $\tilde{\mathcal{M}}_N$ could preserve the cross section data without dip near $u \approx 0$. On the other hand, this term, when combined with the hadronic part $\mathcal{M}_N + \mathcal{M}_{\text{b.g.}}$ via the relative angle $\phi \simeq 90°$, should fill up the rest of the dip, following the meson contribution, while it should reduce the overestimating solid curve to hadronic data in 4(a).

Figure 5 shows the differential cross section $d\sigma/du$ for $\gamma p \to \omega p$ when the cross sections (a) and (b) of Fig. 4 are combined with each other. The parameters $a = -65$ and $b = 93$ are chosen for the relative angle $\phi(u)$ between the hadronic and parton phases of the reaction process in Eq. (13). In actuality, these parameters correspond to $\phi = 0.57\pi$ at $u = -0.15$ GeV^2 which is close to $\phi \simeq 90°$ in the decomposition of the NINA data in Fig. 3. The additional Reggeon $\tilde{\mathcal{M}}_N$ with parton contributions vanishes over $|u| > 2$ GeV^2. The respective roles of the Reggeon $\mathcal{M}_N$

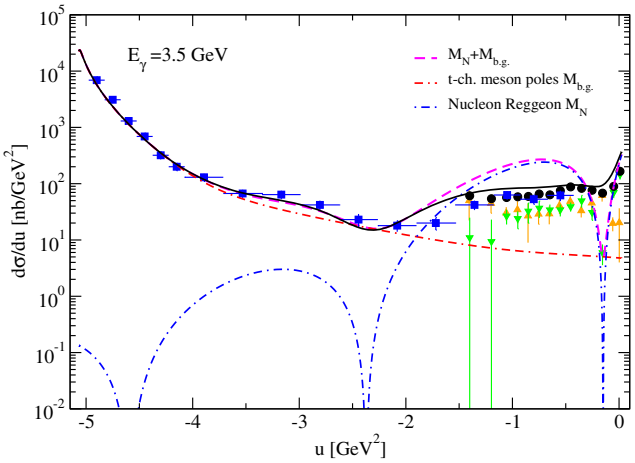

FIG. 5. Differential cross section for $\gamma p \to \omega p$ at $E_\gamma = 3.5$ GeV. The dashed curve corresponds to the solid one in Fig. 4(a). The solid curve from the full amplitude shows a good agreement with data in the overall range of u with the fit of $a = -65$, $b = 93$ for $\phi(u)$. Data are collected from Refs. [9,17].

and the meson exchanges $\mathcal{M}_{\text{b.g.}}$ in the t-channel are depicted by the dash-dotted and dash-dash-dotted curves in order. The rapid increase of cross sections in the CLAS data at large $|u|$ are identified by the t-channel meson exchanges, while the Reggeon $\mathcal{M}_N$ gives the contribution in the backward region $|u| < 2.5$ GeV^2, as expected. We further note that these hadronic contributions $\mathcal{M}_N + \mathcal{M}_{\text{b.g.}}$ reproduce the shape convex up in the interval $-3.5 < u < -2.5$ GeV^2 which was once described by the two quarks exchange in a previous work as elaborated in Ref. [10]. In the current approach, since the dip position of $\tilde{\mathcal{R}}^N$ is removed out to the kinematical region, the term $\tilde{\mathcal{M}}_N$ could play the role to fill up some part of the original dip at $u = -0.15$ GeV^2 as well as to reduce the overestimating contribution of the hadronic part (dashed curve) in Figs. 5 and 6 up to $u \approx -2$ GeV^2, when combined with each other through $\phi \simeq 90°$.

Differential cross sections $d\sigma/du$ at $E_\gamma = 2.8$ and 4.7 GeV are presented in Fig. 6 to show a fair agreement of the present approach with data. The cross section at $E_\gamma = 2.8$ GeV in the upper panel is fitted with $a = -95$ and $b = 70$ and the cross section in the lower panel with $a = -35$ and $b = 120$ for ϕ, respectively. These parameters at $u = -0.15$ GeV^2, for instance, yield $\phi \approx 0.47\pi$ and $\phi \approx 0.7\pi$, in order. Thus, the relative angle ϕ is not quite unique to the energy dependence of cross sections and we have to change the parameters a and b to accomplish such an agreement with data given at different photon energies: $E_\gamma = 2.8$, 3.5, and 4.7 GeV. The contribution of meson exchanges as shown by the dash-dash-dotted curve is responsible for the forward enhancement of the cross section at large $|u|$, as before. The solid curve shows the improvement of the hadronic contribution (dashed curve)

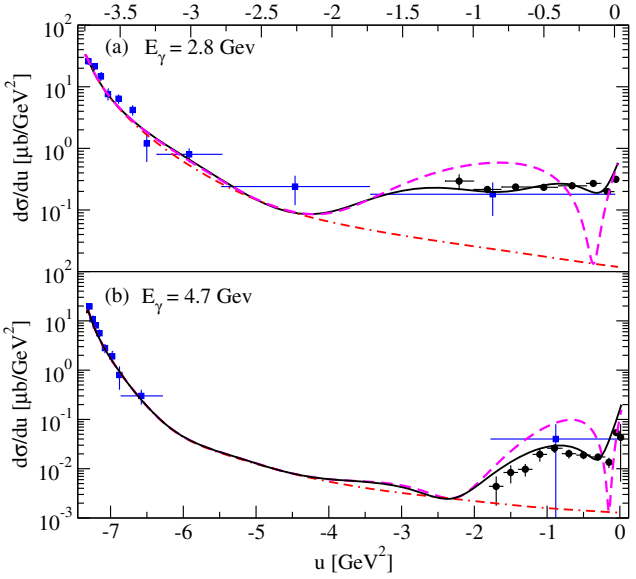

FIG. 6. Differential cross sections $d\sigma/du$ at $E_\gamma = 2.8$ and 4.7 GeV with the parton contributions in Eq. (15) included. The cross section in panel (a) is fitted with $a = -95$, $b = 70$ and in panel (b) with $a = -35$, $b = 120$ for $\phi(u)$. Notations are the same as in Fig. 5. Data are taken from Refs. [17,21].

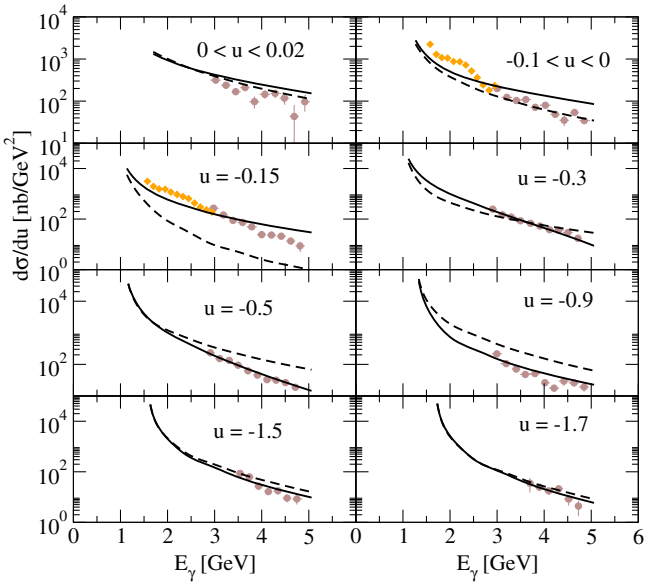

FIG. 7. Energy dependence of differential cross sections $d\sigma/du$. The solid curve is reproduced by a linear fit of data with $a = 31\ \mathrm{GeV}^{-1}E_\gamma - 178$ and $b = 26\ \mathrm{GeV}^{-1}E_\gamma - 0.64$ for the relative angle ϕ. The dashed curve is without parton contributions. The momentum squared u is given in units of GeV^2. Data over $E_\gamma \approx 3$ GeV are taken from Ref. [17] and at low energies are taken from Ref. [18].

by the additional Reggeon $\tilde{\mathcal{M}}_N$ with parton contributions at backward angles.

To test the validity of the present approach further, we check up on the energy dependence of differential cross sections in the range $-1.8 < u < 0.02$ GeV^2 and present the result in Fig. 7. The NINA cross sections $d\sigma/du$ in eight angle bins are reproduced up to photon energy $E_\gamma = 5$ GeV. In the differential cross sections at $-0.1 < u < 0$ and $u = -0.15$ GeV^2 the data recently measured at the SPring-8/LEPS facility [18] are included further for relevance to the present analysis. Since the angle ϕ has the energy dependence as discussed in Figs. 5 and 6, we make parametrized $a = 31\ \mathrm{GeV}^{-1}E_\gamma - 178.2$ and $b = 26\ \mathrm{GeV}^{-1}E_\gamma - 0.64$ for ϕ as a linear function of the photon energy. It is interesting to see the peculiar behavior of the cross section at $u = -0.15$ GeV^2. The improvement of the nucleon Reggeon with partons via the form factor $F^{(s)}$ becomes maximal around the dip position at $u = -0.15$ GeV^2 and vanishes over $u \approx -1.7$ GeV^2, as expected. With an expectation that the exponent x of the As^{-x}-term converted to an effective trajectory $\alpha(u)$, as indicated in Ref. [17], the role of new trajectory $\tilde{\alpha}_N(u)$ with parton contributions is significant at $u = -0.15$ GeV^2, although we do not follow the negative power of x assumed there. The analysis of Fig. 7 is consistent with the observation of Ref. [17] in which the slope of the cross section at $u = -0.15$ GeV^2 is different from others. We obtain a reasonable result in cross sections that cover the overall range of energy and momentum, including NINA data. These findings further support the validity of the present approach.

However, as to the question of true scaling by s^8 power based on the idea that parton contributions remain there to fill up the vanishing of the nucleon Reggeon by the dip, it is hard to agree with their argument in Ref. [17], even though there is no theory at present except for the dimensional counting at $\theta \approx 90°$ to contradict such an experimental observation at such a wide angle $\theta \approx 160°$. This is because our calculation shows that not only the parton contributions but also the t-channel exchanges are needed further in order to fill the dip in the data. In other words, the fact that the dip cannot be filled up without t-channel contributions leads us to speculate that, rather than the recurrence of scaling, it is more related with evidence for the parton distribution inside the target as the photon probe could see by the head-on collision at very backward angles. Our calculation reveals such an aspect through the nucleon form factor with parton densities.

Predictions for differential and total cross sections are presented in Figs. 8 and 9 with the parameters a and b in Fig. 7 for the angle ϕ. The differential cross sections are reproduced in the overall range of $-t$ at the given energy E_γ. In Fig. 8, each cross section at very backward angles reveals the role of the nucleon isoscalar form factor with partons to make the model prediction closer to experimental data, even in the low energy region, less than $E_\gamma = 2$ GeV. Within the present framework it is rather natural that parton contributions via the form factor could appear at lower energies where the nucleon Reggeon is

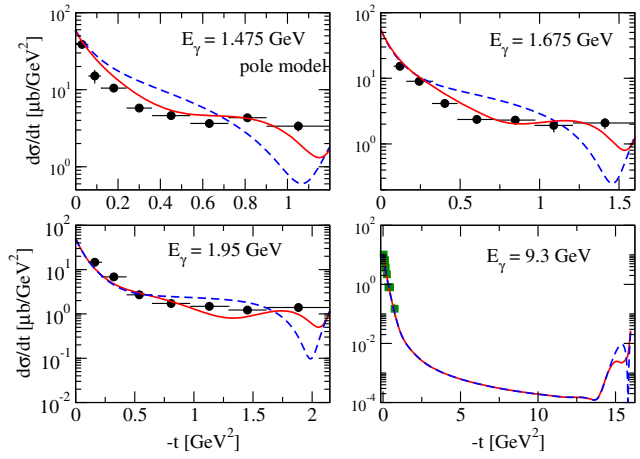

FIG. 8. Differential cross sections for $\gamma p \to \omega p$ in the low energy region below $E_\gamma = 2$ GeV and at high energy $E_\gamma = 9.3$ GeV. Solid curves are from the full calculation with parton contributions. Dashed curves are without parton contributions. Data below 2 GeV are taken from Ref. [25] and data at 9.3 GeV from Ref. [21].

dominant. Such evidence of parton distributions at low energies can be traced out in the total cross section as presented in Fig. 9.

The nucleon isoscalar form factor with parton distributions plays the role to reduce the cross section. Thus, it is a feature of the present approach that the parton distribution could play a role through hadron form factors without the deep scattering of the virtuality photon at high energies. Together with the nucleon Reggeon, a fair agreement with data on total and differential cross sections further confirms

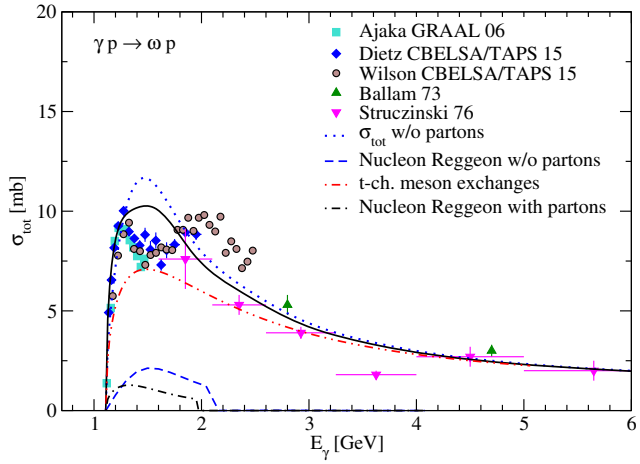

FIG. 9. Total cross section for $\gamma p \to \omega p$. Cross sections $\sigma_{\rm tot}$ with and without parton contributions are given by solid and dotted curves in response to the nucleon contributions with and without the isoscalar form factor which are given by dashed and dash-dotted curves. The background contribution from the t-channel exchange is depicted by the dash-dot-dotted curve. Data are taken from Refs. [21,25–28].

the validity of the background contribution with cutoff masses chosen for the present calculation.

IV. SUMMARY AND DISCUSSIONS

Backward photoproduction of the ω meson off a proton target is investigated within the Regge framework where the nucleon Born terms in the s- and u-channels are Reggeized for the gauge invariant u-channel nucleon Reggeon. The exchanges $\sigma + \pi + f_1 + f_2 +$ Pomeron in the t-channel are included as a background contribution to reproduce reaction cross sections. The cutoff masses for the cutoff functions for $\sigma + \pi + f_1$ poles in the t-channel are determined from natural and unnatural parity cross sections as shown in Fig. 2.

While the N_α trajectory of the nucleon Reggeon reproduces the overall shape of the NINA data measured at the Daresbury Laboratory in the range of $-1.7 < u < 0.02$ GeV^2 and energies at $E_\gamma = 2.8$, 3.5 and 4.7 GeV, a possibility of parton contributions is searched for by considering the nucleon isoscalar form factor at the ωNN vertex which is parametrized in terms of parton distributions. The nucleon Reggeon would make a deep dip at $u = -0.15$ GeV^2, which should be covered over by a fill-up mechanism in order to agree with the cross sections observed in the Daresbury experiment. The dip of the nucleon Reggeon is covered over partly with the meson exchanges and partly with the additional Reggeon with partons at very small $|u|$. This numerical consequence leads to an understanding of the NINA data on the s^8 scaling at angle $\theta \approx 160°$ as being more involved in the observation of parton densities through the backward scattering rather than the scaling which is conventionally known as the energy independence of the cross section at $\theta \approx 90°$. From the practical point of view, a manipulation of the relative phase $\phi \simeq 90°$ and the need of the t-channel contributions are of importance to reproduce the NINA data. Because of the parton densities in the nucleon isoscalar form factor, the parton contributions through the nucleon Reggeon activates rather in the lower energy region than is usually expected, as shown by the description of the total and differential cross sections of GRAAL and CB-ELSA Collaborations.

Confronting the impending 12 GeV upgrade of the CLAS detector, it is timely and interesting to observe in experiments how partons would manifest themselves in the midst of hadronic degrees of freedom and how we could understand such phenomenology through theoretical analysis. In this work we have illustrated how to incorporate parton distributions with hadronic degrees of freedom in hadron models just as the Regge model and the prescription we favored here offer an intuitive way to consider parton contributions in hadron reactions via the hadron form factors. Together with the scaling of meson photoproduction by the factor s^7 around mid angle $\theta = 90°$ observed in the Jefferson Lab, the NINA data at Daresbury, though

almost a 30 year-old issue, provide information to further our understanding of quark dynamics inside hadrons in the limit $-u \approx 0$ that we could expect to observe in future experiments at the 12 GeV upgraded CLAS as well as those facilities LEPS, CB-ELSA, and GRAAL.

ACKNOWLEDGMENTS

This work was supported by the National Research Foundation of Korea Grant No. NRF-2017R1A2B4010117 and partially funded by Grant No. NRF-2016K1A3A7A09005580.

[1] S. J. Brodsky and G. R. Farrar, Phys. Rev. Lett. **31**, 1153 (1973).
[2] H. W. Huang, R. Jakob, P. Kroll, and K. Passek-Kumericki, Eur. Phys. J. C **33**, 91 (2004).
[3] S. V. Goloskokov and P. Kroll, Eur. Phys. J. C **42**, 281 (2005).
[4] B. Dey, Phys. Rev. D **90**, 014013 (2014).
[5] L. Y. Zhu *et al.*, Phys. Rev. Lett. **91**, 022003 (2003).
[6] T. Horn *et al.*, Phys. Rev. Lett. **97**, 192001 (2006).
[7] M. Guidal, M. V. Polyakov, A. V. Radyushkin, and M. Vanderhaeghen, Phys. Rev. D **72**, 054013 (2005).
[8] M. Diehl and P. Kroll, Eur. Phys. J. C **73**, 2397 (2013).
[9] M. Battaglieri *et al.* (CLAS Collaboration), Phys. Rev. Lett. **90**, 022002 (2003).
[10] J.-M. Laget, Phys. Lett. B **489**, 313 (2000).
[11] K.-J. Kong, T. K. Choi, and B.-G. Yu, Phys. Rev. C **94**, 025202 (2016).
[12] B.-G. Yu, H. Kim, and K.-J. Kong, Phys. Rev. D **95**, 014020 (2017).
[13] B.-G. Yu and K.-J. Kong, Phys. Part. Nucl. Lett. **15**, 438 (2018).
[14] B.-G. Yu, T. K. Choi,, and K.-J. Kong, arXiv:1710.04511.
[15] A. Sibirtsev, K. Tsushima, and S. Krewald, arXiv:nucl-th/0202083.
[16] B. Pire, K. Semenov-Tian-Shansky, and L. Szymanowski, Phys. Rev. D **91**, 094006 (2015).
[17] R. W. Clifft, J. B. Dainton, E. Gabathuler, L. S. Littenberg, R. Marshall, S. E. Rock, J. C. Thompson, D. L. Ward, and G. R. Brookes, Phys. Lett. B **72**, 144 (1977).
[18] Y. Morino *et al.*, Prog. Theor. Exp. Phys. (**2015**) 013D01.
[19] M. Battaglieri *et al.*, Phys. Rev. Lett. **87**, 172002 (2001).
[20] M. Guidal, J.-M. Laget, and M. Vanderhaeghen, Nucl. Phys. **A627**, 645 (1997).
[21] J. Ballam, G. B. Chadwick, Y. Eisenberg, E. Kogan, K. C. Moffeit, P. Seyboth, I. O. Skillicorn, H. Spitzer, G. Wolf, H. H. Bingham, W. B. Fretter, W. J. Podolsky, M. S. Rabin, A. H. Rosenfeld, and G. Smadja, Phys. Rev. D **7**, 3150 (1973).
[22] C. F. Perdrisat, V. Punjabi, and M. Vanderhaeghen, Prog. Part. Nucl. Phys. **59**, 694 (2007).
[23] T. K. Choi, K.-J. Kong, and B.-G. Yu, J. Korean Phys. Soc. **67**, 1089 (2015).
[24] M. M. Kaskulov and U. Mosel, Phys. Rev. C **81**, 045202 (2010).
[25] F. Dietz *et al.* (CB-ELSA/TAPS Collaboration), Eur. Phys. J. A **51**, 6 (2015).
[26] A. Wilson *et al.* (CB-ELSA/TAPS Collaboration), Phys. Lett. B **749**, 407 (2015).
[27] J. Ajaka, Y. Assafiri, S. Bouchigny, J. P. Didelez, L. Fichen, M. Guidal, E. Hourany, V. Kouznetsov, R. Kunne, A. N. Mushkarenkov, V. Nedorezov, N. Rudnev, A. Turinge, and Q. Zhao, Phys. Rev. Lett. **96**, 132003 (2006).
[28] W. Struczinski *et al.* (AHHM Collaboration), Nucl. Phys. **B108**, 45 (1976).